Int J Thermophys (2010) 31:416–429
DOI 10.1007/s10765-010-0711-2

Kinetics of Thermal Transformation of $Mg_3(PO_4)_2 \cdot 8H_2O$ to $Mg_3(PO_4)_2$

Banjong Boonchom

Received: 21 December 2008 / Accepted: 30 January 2010 / Published online: 25 February 2010

Abstract The kinetics of thermal dehydration of $Mg_3(PO_4)_2 \cdot 8H_2O$ was investigated using thermogravimetry at four different heating rates. The activation energies of the dehydration step of $Mg_3(PO_4)_2 \cdot 8H_2O$ were calculated through the isoconversional Ozawa and Kissinger-Akahira-Sunose (KAS) methods and iterative methods, which were found to be consistent and indicate a single mechanism. The possible conversion function of the dehydration reaction for $Mg_3(PO_4)_2 \cdot 8H_2O$ has been estimated through the Coats and Redfern integral equation, and a better kinetic model such as random nucleation of the "Avrami–Erofeev equation ($A_{3/2}$ model)" was found. The thermodynamic functions (ΔH^*, ΔG^*, and ΔS^*) of the dehydration reaction are calculated by the activated complex theory and indicate that it is a non-spontaneous process when the introduction of heat is not connected.

Keywords Magnesium phosphates · Non-isothermal decomposition kinetics · Thermodynamic functions

1 Introduction

Thermal decompositions of various compounds are of major importance because they may turn simple compounds into advanced materials, which relate to hydrolysis and dehydration reactions at high temperatures [1–4]. Recently, thermal analysis (TA) methods have been widely used for scientific and practical purposes since they provide reliable information on the physicochemical parameters characterizing the processes of isothermal or non-isothermal decompositions [5]. Studies on such processes have been widely carried out for obtaining fundamental kinetic data, as well as for characterizing the thermodynamic properties of the materials. These data result from the

B. Boonchom (✉)
King Mongkut's Institute of Technology Ladkrabang, Chumphon Campus, 17/1 M. 6,
Pha Thiew District, Chumphon 86160, Thailand
e-mail: kbbajon@kmitl.ac.th; bjbchem@yahoo.com

great variety of factors with diverse effects (reconstruction of solid-state crystal lattices, formation and growth of new crystallization nuclei, diffusion of gaseous reagents or reaction products, materials heat conductance, static or dynamic character of the environment, physical state of the reagents—dispersity, layer thickness, specific area and porosity, type, amount and distribution of the active centers on solid-state surface, etc.) [1,4]. The results obtained on these bases can be directly applied in materials science for the preparation of various metals and alloys, cements, ceramics, glasses, enamels, glazes, polymers, and composite materials.

$Mg_3(PO_4)_2 \cdot 8H_2O$ and its decomposed product $Mg_3(PO_4)_2$ have been used in several fields of industry, for example, in agricultural, pharmaceutical, food, and textile industries because their main properties are insolubility in water, high temperature resistance, chemical stability, and ecologically (toxicologically) harmful elements [1,2]. Consequently, the thermodynamic (ΔH^*, ΔS^*, ΔG^*) and kinetic (E, A, mechanism and model) parameters of the dehydration reaction of $Mg_3(PO_4)_2 \cdot 8H_2O$ have attracted the interest of thermodynamic and kinetic scientists. In this respect, the kinetics and thermodynamics of thermal transformation of $Mg_3(PO_4)_2 \cdot 8H_2O$ to $Mg_3(PO_4)_2$ were investigated in this study using Ozawa [6], Kissinger-Akahira-Sunose [7,8], and iterative methods [9]. The best possible conversion functions have been estimated using the Coats and Redfern method which give the best description of the studied dehydration process and allows the calculation of reliable values of the kinetic triplet parameter [10]. These types of kinetic and thermodynamic treatments have never been reported in the literature.

2 Experimental

2.1 Materials and Measurement

$Mg_3(PO_4)_2 \cdot 8H_2O$ crystalline powder (34,470-2; 99 mass%) was commercially obtained from Aldrich Co. Ltd, and was used without further purification. The characterization and identification of $Mg_3(PO_4)_2 \cdot 8H_2O$ and its final decomposition product $Mg_3(PO_4)_2$ were carried out by X-ray powder diffraction (Siemens D500 diffractometer), an infrared spectrophotometer (Bonen MB-100 FTIR), and a scanning electron microscope (JEOL JSM-5400) [2]. Thermal analysis measurements [thermogravimetry (TG); differential thermogravimetry (DTG); and differential thermal analysis (DTA)] were carried out on a Pyris Diamond Perkin Elmer apparatus by increasing the temperature from 303 K to 1273 K with calcined $\alpha - Al_2O_3$ powder as the reference. The experiments were performed in air atmosphere at heating rates of (5, 10, 15, and 20) $K \cdot min^{-1}$. The sample mass was kept at about 6.0 mg to 10.0 mg in an alumina crucible without pressing.

3 Results and Discussion

3.1 Thermal Analysis

TG–DTG–DTA curves of the thermal decomposition of $Mg_3(PO_4)_2 \cdot 8H_2O$ at a heating rate of $10\,K \cdot min^{-1}$ are shown in Fig. 1. The TG curve shows a major

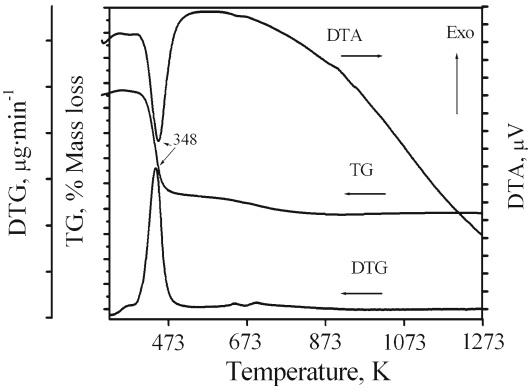

Fig. 1 TG–DTG–DTA curves of $Mg_3(PO_4)_2 \cdot 8H_2O$ in air at heating rate of $10\,K \cdot min^{-1}$

decomposition step in the range of 373 K to 523 K, which relates to the mass loss of 32.19 % (7.28 mol H_2O). A minor mass loss is observed in the range of 573 K to 723 K, which corresponds to a mass loss of 3.00 % (0.68 mol H_2O). The total mass loss is 35.19 % (7.96 mol H_2O), which agrees with the theoretical value for $Mg_3(PO_4)_2 \cdot 8H_2O$ (36.14 %, 8.00 mol H_2O). DTA and DTG curves show temperature peaks at 348 K and 683 K, which closely correspond to the mass loss observed in the TG trace. The retained mass of about 64.81 % is compatible with the value expected for the formation of $Mg_3(PO_4)_2$, which is verified by XRD and FTIR measurements [2]. The overall reaction is

$$Mg_3(PO_4)_2 \cdot 8H_2O \longrightarrow Mg_3(PO_4)_2\,0.68H_2O + 7.28H_2O \quad (1)$$

$$Mg_3(PO_4)_2 \cdot 0.68H_2O \longrightarrow Mg_3(PO_4)_2 + 0.68H_2O \quad (2)$$

Therefore, the temperature at which the theoretical mass loss is achieved, can also determined from the TG curve and is considered to be the minimum temperature needed for the calcination process. Thus, the $Mg_3(PO_4)_2 \cdot 8H_2O$ sample was calcined at 773 K for 2 h in the furnace, and its final decomposition product, $Mg_3(PO_4)_2$ was obtained [2].

3.2 Kinetic Studies

3.2.1 Calculation of the Activation Energy by Isoconversional Methods

Decomposition of crystal hydrates is a solid-state process of the type [11–15]: A (solid) → B (solid) + C (gas). The kinetics of such reactions is described by various equations taking into account the special features of their mechanisms. The reaction can be expressed through the temperatures corresponding to fixed values of the extent of conversion ($\alpha = (m_i - m_a)/(m_i - m_f)$, where m_i, m_a, and m_f are the initial, actual, and final sample masses at time t) from experiments at different heating rates (β);

$$\frac{d\alpha}{dt} = k(T)\,f(\alpha). \quad (3)$$

The temperature dependence of the rate constant k for the process is described by the Arrhenius equation:

$$k = A \exp\left(-\frac{E}{RT}\right) \tag{4}$$

where A is the pre-exponential factor (s^{-1}), E is the apparent activation energy ($kJ \cdot mol^{-1}$), T is the absolute temperature (K), and R is the universal gas constant ($8.314\ kJ \cdot mol^{-1} \cdot K^{-1}$). Substitution of Eq. 4 in Eq. 3 gives

$$\frac{d\alpha}{dt} = A \exp\left(-\frac{E}{RT}\right) f(\alpha) \tag{5}$$

When the temperature increases at a constant rate,

$$\frac{d\alpha}{dT} = \beta = \text{const}, \tag{6}$$

Therefore,

$$\frac{d\alpha}{dT} = \frac{A}{\beta} \exp\left(-\frac{E}{RT}\right) f(\alpha) \tag{7}$$

$$g(\alpha) = \int_0^\alpha \frac{d(\alpha)}{f(\alpha)} = \frac{A}{\beta} \int_0^T \exp\left(-\frac{E}{RT}\right) dT \tag{8}$$

The conversion function $f(\alpha)$ for a solid-state reaction depends on the reaction mechanism. The solutions of the left-hand side integral depend on the explicit expression of the function $f(\alpha)$ and are denoted as $g(\alpha)$. The formal expressions of the functions $g(\alpha)$ depend on the conversion mechanism and its mathematical model. The latter usually represents the limiting stage of the reaction—the chemical reactions; random nucleation and nuclei growth; and phase boundary reaction or diffusion. Algebraic expressions of functions of the most common reaction mechanisms operating in solid-state reactions are presented in Table 1 [11–15].

The activation energy (E_α) can be calculated according to isoconversional methods. In kinetic studies of $Mg_3(PO_4)_2 \cdot 8H_2O$, the Ozawa [6] and the Kissinger-Akahira-Sunose (KAS) [7,8] equations were used to determine the activation energy of the dehydration reaction in only the first step (Eq. 1). The second dehydration step is a very fast mass loss over short temperature ranges. The obtained data in this step will be highly sensitive to non-isothermal kinetics analysis errors.

The equations used for E_α calculation are

Ozawa equation:

$$\ln \beta = \ln\left(\frac{AE_\alpha}{Rg(\alpha)}\right) - 5.3305 - 1.0516\left(\frac{E_\alpha}{RT}\right) \tag{9}$$

Table 1 Algebraic expressions of functions $g(\alpha)$ and $f(\alpha)$ and their corresponding mechanisms [5,9,11–13]

No.	Symbol	Name of the function	$f(\alpha)$	g(α)	Rate-determination mechanism
1. Chemical process of mechanism non-invoking equations					
1	$F_{1/3}$	One-third order	$(3/2)(1-\alpha)^{2/3}$	$[1-(1-\alpha)^{1/3}]$	Chemical reaction
2	$F_{3/4}$	Three-quarters order	$4(1-\alpha)^{3/4}$	$[1-(1-\alpha)^{1/4}]$	Chemical reaction
3	$F_{3/2}$	One and a half order	$2(1-\alpha)^{3/2}$	$[1-(1-\alpha)^{-1/2}-1]$	Chemical reaction
4	F_2	Second order	$(1-\alpha)^2$	$(1-\alpha)^{-1}-1$	Chemical reaction
5	F_n	n-th order kinetics ($n \pm 1$)	$(1-\alpha)^n$	$[1-(1-\alpha)^{1-n}]/(1-n)$	Chemical reaction
2. Acceleratory equations					
6	$P_{3/2}$	Mampel power law	$(2/3)\alpha^{-1/2}$	$\alpha^{3/2}$	Nucleation
7	$P_{1/2}$	Mampel power law	$2\alpha^{1/2}$	$\alpha^{1/2}$	Nucleation
8	$P_{1/3}$	Mampel power law	$3\alpha^{2/3}$	$\alpha^{1/3}$	Nucleation
9	$P_{1/4}$	Mampel power law	$4\alpha^{3/4}$	$\alpha^{1/4}$	Nucleation
3. Sigmoid rate equations or random nucleation and subsequent growth					
10	A_1, F_1	Avrami–Erofeev equation	$(1-\alpha)$	$-\ln(1-\alpha)$	Assumed random nucleation and its subsequent growth, $n=1$
11	$A_{3/2}$	Avrami–Erofeev equation	$(3/2)(1-\alpha)[-\ln(1-\alpha)]^{1/3}$	$[-\ln(1-\alpha)]^{2/3}$	Assumed random nucleation and its subsequent growth, $n=1.5$
12	A_2	Avrami–Erofeev equation	$2(1-\alpha)[-\ln(1-\alpha)]^{1/2}$	$[-\ln(1-\alpha)]^{1/2}$	Assumed random nucleation and its subsequent growth, $n=2$
13	A_4	Avrami–Erofeev equation	$4(1-\alpha)[-\ln(1-\alpha)]^{3/4}$	$[-\ln(1-\alpha)]^{1/4}$	Assumed random nucleation and its subsequent growth, $n=4$
4. Deceleratory rate equations					
4.1 Phase boundary reaction					
14	R_1, F_0, P_1	Power law	$(1-\alpha)^0$	α	One-dimensional advance of the reaction interface, power law or zero-order kinetics
15	$R_2, F_{1/2}$	Power law	$2(1-\alpha)^{1/2}$	$[1-(1-\alpha)^{1/2}]$	Contracting area (cylindrical symmetry) or one-half-order
16	R_3,$F_{2/3}$	Power law	$3(1-\alpha)^{2/3}$	$[1-\ln(1-\alpha)]^{1/3}$	Contracting volume (spherical symmetry) or two-thirds order

Table 1 continued

No.	Symbol	Name of the function	$f(\alpha)$	$g(\alpha)$	Rate-determination mechanism
4.2 Based on the diffusion					
17	D_1	Parabola law ($\alpha = kt^{1/2}$)	$1/2\alpha$	α^2	One-dimension diffusion
18	D_2	Valensi equation	$[-\ln(1-\alpha)]^{-1}$	$\alpha + (1-\alpha)\ln(1-\alpha)$	Two-dimension diffusion
19	D_3	Jander equation	$(3/2)(1-\alpha)^{2/3}/[1-(1-\alpha)^{1/3}]$	$[1-(1-\alpha)^{1/3}]^2$	Three-dimension diffusion
20	D_4	Ginstling–Brounstein Eq.	$(3/2)(1-\alpha)^{-1/3}-1]^{-1}$	$[1-(2/3)\alpha-(1-\alpha)^{2/3}]$	Three-dimension diffusion
21	D_5	Zhuravlev Lesokhin Tempelman Eq.	$(3/2)(1-\alpha)^{4/3}/[1-(1-\alpha)^{-1/3}]$	$[(1-\alpha)^{-1/3}-1]^2$	Three-dimension diffusion
22	D_6	Komastsu-Uemura or anti-Jander Eq.	$(3/2)(1+\alpha)^{2/3}/[(1+\alpha)^{1/3}-1]$	$[(1+\alpha)^{1/3}-1]^2$	Three-dimension diffusion

KAS equation:

$$\ln\left(\frac{\beta}{T^2}\right)_\alpha = \ln\left(\frac{AE}{g(\alpha)R}\right) - \left(\frac{E_\alpha}{RT}\right) \tag{10}$$

The Arrhenius parameters, together with the reaction model, are sometimes called the kinetic triplet. $g(\alpha) = \int_0^\alpha \mathrm{d}(\alpha)/f(\alpha)$ is the integral form of $f(\alpha)$, which is the reaction model that depends on the reaction mechanism. According to the Ozawa (9) and the KAS (10) equations, the activation energies of the different stages do not depend on the reaction mechanism and the shape of the $g(\alpha)$ function. An iterative procedure is used to calculate the approximate value of E approach to the exact value, according to the following equations [5,9,11,12]:

Iterative method I:

$$\ln\left(\frac{\beta}{H(x)}\right) = \ln\left(\frac{AE_\alpha}{Rg(\alpha)}\right) - 5.3305 - 1.0516\left(\frac{E_\alpha}{RT}\right) \tag{11}$$

Iterative method II:

$$\ln\left(\frac{\beta}{h(x)T^2}\right) = \ln\left(\frac{AE_{\alpha 1}}{g(\alpha)R}\right) - \left(\frac{E_{\alpha 1}}{RT}\right) \tag{12}$$

where $H(x)$ or $h(x)$ is expressed by the fourth Senum and Yang approximation formulae [5,9,16]:

$$H(x)\,\text{or}\,h(x) = \frac{x^4 + 18x^3 + 88x^2 + 96x}{x^4 + 20x^3 + 120x^2 + 240x + 120} \tag{13}$$

where $x = E_\alpha/RT$ and E_α is the average activation energy from the KAS method.

The iterative procedure is as follows: (i) suppose $h(x) = 1$ to estimate the initial value of the activation energy $E_{\alpha 1}$. The conventional isoconversional methods stop the calculation at this step; (ii) using $E_{\alpha 1}$ to calculate $h(x)$, then from Eqs. 11 and 12 to calculate a new value of $E_{\alpha 2}$ for the activation energy from the plot of $\ln[\beta/h(x)T^2]$ versus $1/T$; (iii) repeat step (ii), replacing $E_{\alpha 1}$ with $E_{\alpha 2}$. When $E_{\alpha 1} - E_{\alpha 2} < 0.1\,\text{kJ}\cdot\text{mol}^{-1}$, the last value of $E_{\alpha 1}$ is the exact value of the activation energy of the reaction. The plot is model independent since the estimation of the apparent activation energy does not require selection of a particular kinetic model (type of $g(\alpha)$ function), which indicates that the activation energy values are usually regarded as more reliable than these obtained by a single TG curve.

According to the linear isoconversional method, the basic data of α and T collected from the TG curves (Fig. 1) of the decomposition step of $Mg_3(PO_4)_2 \cdot 8H_2O$ at various heating rates ($5\,\text{K}\cdot\text{min}^{-1}$, $10\,\text{K}\cdot\text{min}^{-1}$, $15\,\text{K}\cdot\text{min}^{-1}$, and $20\,\text{K}\cdot\text{min}^{-1}$) are plotted in Fig. 2. According to Eqs. 8–11, the plots of $\ln\beta$ versus $1000T^{-1}$ (Ozawa), $\ln\beta/T^2$ versus $1000T^{-1}$ (KAS), $\ln(\beta h(x)^{-1}T^{-2})$ versus $1000T^{-1}$ (iterative method I), and $\ln(\beta H(x)^{-1})$ versus $1000T^{-1}$ (iterative method II) corresponding to different conversions α can be obtained by a linear regression of the least-squares method, respectively. The activation energies E_α and the standard deviations of E values can be calculated

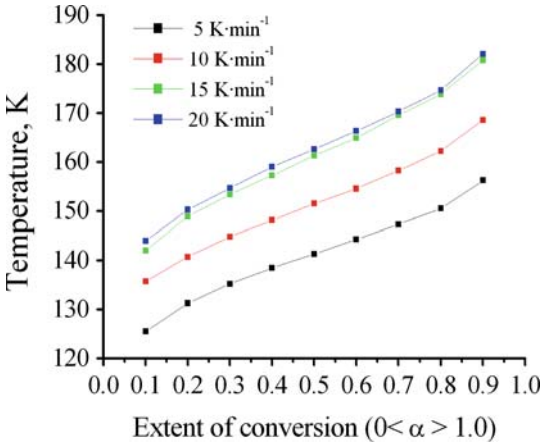

Fig. 2 Plots of α versus T at four heating rates ((5, 10, 15, and 20) $\mathrm{K \cdot min^{-1}}$)

from the slopes of the straight lines with a better linear correlation coefficient (r^2) in the α range of 0.2 to 0.8. As shown in Table 2, the activation energy values calculated by all methods are close to each other. If E_α values are independent of α, the decomposition may be a simple reaction, while the dependence of E_α on α should be interpreted in terms of multi-step reaction mechanisms [12–15]. Neglecting the dependence of E versus α, average values of $E_\alpha = (86.61 \pm 1.14)\,\mathrm{kJ \cdot mol^{-1}}$ (iterative method I) and $(90.28 \pm 1.17)\,\mathrm{kJ \cdot mol^{-1}}$ (iterative method II) are obtained. It was considered that the E_α values are independent of α if the relative errors of the slopes of Iterative I and II equations straight lines were less than 10 % (SD $\leq$ 3.25). The activation energy values calculated by all methods are close to each other. Then, it can be concluded that the activation energy values obtained from different methods are more reliable and these methods can be used in the determination of the activation energy values with satisfactory accuracy. For the dehydration reaction of $Mg_3(PO_4)_2 \cdot 8H_2O$, the activation energy values change little with α, so this process could be a single kinetic mechanism, corresponding to an endothermic peak at 348 K on the DTA curve. The activation energy for the release of the water of crystallization lie in the range of $60\,\mathrm{kJ \cdot mol^{-1}}$ to $90\,\mathrm{kJ \cdot mol^{-1}}$, while the values for coordinately bounded decomposition are within the range of $130\,\mathrm{kJ \cdot mol^{-1}}$ to $160\,\mathrm{kJ \cdot mol^{-1}}$ [13–15]. In addition, the water eliminated at 423 K and below can be considered as water of crystallization, whereas water eliminated at 573 K and above indicates its co-ordination by the metal atom. The calculated activation energies from all methods for the dehydration reaction lie in the range of $80\,\mathrm{kJ \cdot mol^{-1}}$ to $100\,\mathrm{kJ \cdot mol^{-1}}$ whereas the decomposition stage of $Mg_3(PO_4)_2 \cdot 8H_2O$ is observed in the temperature range of 400 K to 523 K. On the basis of these results, the dehydration reaction of the studied compound may be related with the crystallization of water molecules inside this compound (Eq. 1).

3.2.2 Determination of the Most Probable Mechanism and the Pre-Exponential Factor

Several authors [10,13–16] suggested different ways to solve the right-hand side integral in Eq. 8. For the present study, one calculation procedure was based on the Coats

Table 2 Activation energies (E_α) and correlation coefficient (r^2) for the dehydration of $Mg_3(PO_4)_2 \cdot 8H_2O$ at different heating rates ((5, 10, 15, and 20) $K \cdot min^{-1}$) from different methods

α	Ozawa method			KAS method			$\ln(\beta)/(h(x)T^2)$			$\ln(\beta)/(H(x))$		
	E_α ($kJ \cdot mol^{-1}$)	SD	r^2	E_α ($kJ \cdot mol^{-1}$)	SD	r^2	E_α ($kJ \cdot mol^{-1}$)	SD	r^2	E_α ($kJ \cdot mol^{-1}$)	SD	r^2
0.2	91.66	1.70	0.9802	100.85	1.28	0.9816	89.93	1.25	0.9789	94.92	1.75	0.9815
0.3	91.53	1.65	0.9789	100.37	1.10	0.984	90.62	1.52	0.9801	94.74	1.69	0.9803
0.4	88.78	0.61	0.9816	92.06	2.04	0.9794	89.76	1.19	0.9733	92.02	0.66	0.9828
0.5	85.88	0.48	0.9761	97.37	0.03	0.9789	86.68	0.03	0.9771	89.15	0.43	0.9778
0.6	84.00	1.19	0.9754	95.46	0.76	0.9725	84.69	0.73	0.9741	87.31	1.12	0.9772
0.7	85.07	0.79	0.9677	98.44	0.37	0.9738	82.58	1.52	0.9666	87.02	1.23	0.9776
0.8	83.20	1.50	0.9691	97.64	0.07	0.9773	82.01	1.74	0.9648	86.81	1.31	0.9745
Av.	87.16	1.13	0.9868	97.46	0.81	0.9782	86.61	1.14	0.9736	90.28	1.17	0.9788

Av. average value, *SD* standard deviation

and Redfern equation [10]. Data from TG curves (Fig. 2) in the decomposition range $0.2 < \alpha < 0.8$ were used to determine the kinetic parameters of the process in all calculation procedures. The integral method of Coats and Redfern has been successfully used for studying the kinetics of dehydration and decomposition of different solid substances [13–16]. The kinetic parameters can be derived using a linear form of the modified Coats and Redfern equation:

$$\ln\left(\frac{g(\alpha)}{T^2}\right) = \ln\left(\frac{AR}{\beta E_\alpha}\right)\left(1-\frac{2RT}{E_\alpha}\right) - \left(\frac{E_\alpha}{RT}\right) \cong \ln\left(\frac{AR}{\beta E_\alpha}\right) - \left(\frac{E_\alpha}{RT}\right) \quad (14)$$

Hence, $\ln\left(\frac{g(\alpha)}{T^2}\right)$ calculated for the different α values at the single β value on $1000/T$ must give rise to a single master straight line, so the activation energy and the pre-exponential factor can be calculated from the slope and intercept through an ordinary least-squares estimation. The activation energy, pre-exponential factor, and the correlation coefficient can be calculated from the equation of Coats and Redfern combined with 22 conversion functions (Table 1) [13–16]. Comparing the kinetic parameters from the Coats and Redfern equation, the probable kinetic model may be selected, for which the values of E_α and A were calculated with a better linear correlation coefficient and the activation energies obtained from the Coats and Redfern equation above were showing good agreement with those obtained from the iterative procedure or KAS or Ozawa methods with a better correlation coefficient (r^2). So the pre-exponential factor A can be obtained by calculating the average value of A (s^{-1}) from Eq. 14 for different heating rates.

Equation 14 was used to estimate the most correct mechanism, i.e., $g(\alpha)$ and $f(\alpha)$ functions. The activation energy, pre-exponential factor, and the correlation coefficient can be calculated from the Coats and Redfern equation combined with 22 conversion functions (Table 1) [5,9,11–15]. The most probable mechanism function was assumed to be the one for which the value of the correlation coefficient was higher and the activation energies calculated by the Coats and Redfern method were close to the optimized values from the iterative methods. The optimized values from the Coats and Redfern method are the data of the activation energy and pre-exponential factor; those were calculated with the best equation and are shown in Table 3. According to Table 3, it was seen that the activation energy values calculated by the iterative methods were close to the optimized values from the Coats and Redfern method, and the respective correlation coefficients are preferable. This is considered sufficient to conclude that the non-isothermal kinetic parameters of the dehydration reaction of $Mg_3(PO_4)_2 \cdot 8H_2O$ can be reliably calculated with correctly chosen $g(\alpha)$ and $f(\alpha)$ functions. Based on these results, we can draw a conclusion that the obtained possible conversion function is the $A_{3/2}$ model (sigmoidal rate equations or random nucleation and subsequent growth) for the dehydration of $Mg_3(PO_4)_2 \cdot 8H_2O$, and the corresponding functions are $f(\alpha) = (3/2)(1-\alpha)[-\ln(1-\alpha)]^{1/3}$ and $g(\alpha) = -\ln(1-\alpha)]^{2/3}$. The correlated kinetic parameters are $E_\alpha = (82.17 \pm 6.51)\ \mathrm{kJ \cdot mol^{-1}}$ and $A = (5.54 \times 10^2 \pm 23.0)\ \mathrm{s^{-1}}$. Based on the values of the activation energy and pre-exponential factor, the strengths of binding of water molecules in the crystal lattice are different and, hence, result in different dehydration temperatures and kinetic parameters [11–15]. The activation

Table 3 Kinetics parameters obtained from different $f(\alpha)$ by the Coats–Redfern method at different heating rates ($\beta = (5, 10, 15, \text{and } 20)\,\text{K}\cdot\text{min}^{-1}$)

No.	Model	Coats–Redfern method				
		E_α (kJ · mol^{-1})		A (s^{-1})		r^2
		E_α	±Error	A	±Error	
1	$F_{1/3}$	32.92	3.27	2.03×10^{-3}	5.31	0.9751
2	$F_{3/4}$	12.01	1.64	1.22×10^{-5}	2.84	0.9281
3	$F_{3/2}$	62.39	5.53	5.63	4.94	0.9660
4	F_2	178.59	14.86	1.76×10^{14}	3.67×10^{2}	0.9987
5	$F_n(n = 3)$	243.10	19.75	3.37×10^{22}	2.23×10^{3}	0.9910
6	$P_{3/2}$	132.79	11.59	1.19×10^{8}	1.08×10^{2}	0.9674
7	$P_{1/2}$	39.53	3.97	9.86×10^{-3}	6.75	0.9589
8	$P_{1/3}$	23.99	2.70	3.47×10^{-4}	4.23	0.9503
9	$P_{1/4}$	16.87	3.12	7.90×10^{-5}	3.15	0.9387
10	A_1	125.84	10.83	5.61×10^{7}	8.50×10	0.9944
11	$\mathbf{A_{3/2}}$	**82.17**	**6.51**	$\mathbf{5.54} \times 10^{2}$	$\mathbf{2.30} \times \mathbf{10}$	**0.9940**
12	A_2	59.37	5.50	2.12	1.04×10	0.9935
	A_2	37.21	3.72	6.34×10^{-3}	3.05	0.9926
13	A_4	26.14	2.83	9.09×10^{-4}	4.46	0.9914
14	R_1	86.16	7.78	7.88E+02	2.46×10	0.9655
15	R_2	104.39	9.18	1.32×10^{5}	2.43×10	0.9836
16	R_3	111.18	9.71	9.11×10^{5}	2.54×10^{-1}	0.9879
17	D_1	179.42	15.39	2.29×10^{13}	4.30×10^{2}	0.9683
18	D_2	201.87	17.13	1.43×10^{16}	8.15×10^{2}	0.9791
19	D_3	229.45	19.25	1.28×10^{19}	1.78×10^{3}	0.9887
20	D_4	210.98	17.83	6.45×10^{16}	1.05×10^{3}	0.4909
21	D_5	54.52	4.89	9.20×10^{-1}	9.71	0.9425
22	D_6	11.56	1.65	1.83×10^{-5}	2.82	0.9929

The bold values estimated by the modified coats and Redfern equation were the most probable mechanism function

energy of the dehydration reaction calculated by using the $A_{3/2}$ model (Table 3) suggests that the hydrates in the studied compound are the crystallization of water in the structure. The pre-exponential factor (A) values in the Arrhenius equation for solid-phase reactions are expected to be in a wide range (six or seven orders of magnitude), even after the effect of the surface area is taken into account [17–19]. The low factors will often indicate a surface reaction, but if the reactions are not dependent on the surface area, the low factor may indicate a "tight" complex. The high factors will usually indicate a "loose" complex [17–19]. Even higher factors (after correction for the surface area) can be obtained for complexes having free translation on the surface. Since the concentrations in solids are not controllable in many cases, it would

have been convenient if the magnitude of the pre-exponential factor is indicated for reaction molecularity. On the basis of these reasons, the thermal dehydration reaction of $Mg_3(PO_4)_2 \cdot 8H_2O$ may be interpreted as "tight complexes." This result is consistent with thermal analysis, which confirms that the decomposition product is magnesium pyrophosphate ($Mg_3(PO_4)_2$).

3.3 Determination of the Thermodynamic Functions

From the activated complex theory (transition state) of Eyring [17–19], the following general equation may be written:

$$A = \left(\frac{e\chi k_B T_p}{h}\right) \exp\left(\frac{\Delta S^*}{R}\right) \tag{15}$$

where A is the pre-exponential factor A obtained from the Coats and Redfern method; e is 2.7183, the Neper number; χ is the transition factor, which is unity for monomolecular reactions; k_B is the Boltzmann constant; h is the Planck constant; and T_p is the peak temperature of the DTA curve. The change of the entropy may be calculated according to the formula:

$$\Delta S^* = R \ln\left(\frac{Ah}{e\chi k_B T_p}\right) \tag{16}$$

Then

$$\Delta H^* = E^* - RT_p, \tag{17}$$

when E^* is the activation energy E_α obtained from the Coats and Redfern method. The changes of the enthalpy ΔH^* and Gibbs free energy ΔG^* for the activated complex formation from the reagent can be calculated using the well-known thermodynamic equation:

$$\Delta G^* = \Delta H^* - T_p \Delta S^*. \tag{18}$$

The heat of activation (ΔH^*), entropy of activation (ΔS^*), and free energy of activation decomposition (ΔG^*) were calculated at $T = T_p$ (T_p is the DTA peak temperature at the corresponding stage), since this temperature characterizes the highest rate of the process, and therefore, is the important parameter.

The calculated values of ΔH^*, ΔS^*, and ΔG^* for the dehydration step of $Mg_3(PO_4)_2 \cdot 8H_2O$ are $78.58\,kJ \cdot mol^{-1}$, $-203.79\,J \cdot mol^{-1} \cdot K^{-1}$, and $166.56\,kJ \cdot mol^{-1}$, respectively. The entropy of activation (ΔS^*) value for the dehydration step is negative. It means that the corresponding activated complexes have a higher degree of arrangement than the initial state. Since the decomposition of $Mg_3(PO_4)_2 \cdot 8H_2O$ proceeds as a single reaction, the formation of the activated complex passed *in situ*. In terms of the activated complex theory (transition theory) [9,17–23], a positive value of

$\Delta S*$ indicates a malleable activated complex that leads to a large number of degrees of freedom of rotation and vibration. This result may be interpreted as a "fast" stage. On the other hand, a negative value of $\Delta S*$ indicates a highly ordered activated complex, and the degrees of freedom of rotation as well as of vibration are less than they are in the non-activated complex. These results may indicate a "slow" stage. Therefore, the dehydration reaction of $Mg_3(PO_4)_2 \cdot 8H_2O$ may be interpreted as a "slow" stage [9,17–23]. The positive value of the enthalpy $\Delta H*$ is in good agreement with endothermic effects in DTA data. The positive values of $\Delta H*$ and $\Delta G*$ for the dehydration stage show that it is connected with the introduction of heat and it is a non-spontaneous process. These thermodynamic functions are consistent with kinetic parameters and thermal analysis data.

4 Conclusions

The dehydration reaction of $Mg_3(PO_4)_2 \cdot 8H_2O$ is important for further treatment. The kinetics of the thermal decomposition of $Mg_3(PO_4)_2 \cdot 8H_2O$ was studied using non-isothermal TG applying a model-fitting method. The activation energies calculated for the dehydration step of $Mg_3(PO_4)_2 \cdot 8H_2O$ by different methods and techniques were found to be consistent and indicate a single mechanism. This indicates that the activation energy of dehydration is independent of the process and the nature of non-isothermal methods as well as of TGA. On the basis of correctly established values of the apparent activation energy, pre-exponential factor, and the changes of entropy, enthalpy, and Gibbs free energy, certain conclusions can be made concerning the mechanisms and characteristics of the processes.

Acknowledgments The author thanks the Chemistry and Physics Departments, Khon Kaen University for providing research facilities. This work is financially supported by the Thailand Research Fund (TRF) and the Commission on Higher Education (CHE): Research Grant for New Scholar, Ministry of Education, Thailand.

References

1. Ž. Mesíková, P. Šulcová, M. Trojan, J. Therm. Anal. Cal. **88**, 103 (2007)
2. M.A. Aramendía, V. Borau, C. Jiménez, J.M. Marinas, F.J. Romero, J. Colloid Interf. Sci. **217**, 288 (1999)
3. B. Boonchom, S. Maensiri, C. Danvirutai, Mater. Chem. Phys. **109**, 404 (2008)
4. C.-M. Wang, H.-C. Liau, W.-T. Tsai, Mater. Chem. Phys. **102**, 207 (2007)
5. G.I. Senum, R.T. Yang, J. Therm. Anal. **11**, 445 (1977)
6. T. Ozawa, Bull. Chem. Soc. Jpn. **38**, 1881 (1965)
7. H.E. Kissinger, J. Anal. Chem. **29**, 1702 (1957)
8. T. Akahira, T. Sunose, Res. Report Chiba Inst. Technol. (Sci. Technol.) **16**, 22 (1971)
9. Z. Gao, M. Nakada, I. Amasaki, Thermochim. Acta **369**, 137 (2001)
10. A.W. Coats, J.P. Redfern, Nature **20**, 68 (1964)
11. T. Vlase, G. Vlase, M. Doca, N. Doca, J. Therm. Anal. Cal. **72**, 597 (2003)
12. L.T. Vlaev, M.M. Nikolova, G.G. Gospodinov, J. Solid State Chem. **177**, 2663 (2004)
13. X. Gao, D. Dollimore, Thermochim. Acta **215**, 47 (1993)
14. M.A. Gabal, Thermochim. Acta **402**, 199 (2003)
15. K. Zhang, J. Hong, G. Cao, D. Zhan, Y. Tao, C. Cong, Thermochim. Acta **437**, 145 (2005)
16. G. Chumxiu, S. Yufang, C. Donghua, J. Therm. Anal. Cal. **76**, 203 (2004)

17. J. Ŝesták, *Thermodynamical Properties of Solids* (Academia, Prague, 1984)
18. D. Young, *Decomposition of Solids* (Pergamon Press, Oxford, 1966)
19. H.M. Cordes, J. Phys. Chem. **72**, 2185 (1968)
20. J.M. Criado, L.A. Pérez-Maqueda, P.E. Sánchez-Jiménez, J. Therm. Anal. Cal. **82**, 671 (2005)
21. B. Boonchom, J. Chem. Eng. Data **53**, 1553 (2008)
22. L. Vlaev, N. Nedelchev, K. Gyurova, M. Zagorcheva, J. Anal. Appl. Pyrol. **81**, 253 (2008). References therein
23. T. Vlase, G. Vlase, N. Birta, N. Doca, J. Therm. Anal. Cal. **88**, 631 (2007)